Hindawi
Journal of Sensors
Volume 2023, Article ID 1282309, 12 pages
https://doi.org/10.1155/2023/1282309

Research Article

eMeD: An Experimental Study of an Autonomous Wearable System with Hybrid Energy Harvester for Internet of Medical Things

Yung-Wey Chong,[1] **Widad Ismail**,[2] **and Kok-Lim Alvin Yau**[3]

[1]*National Advanced IPv6 Centre, Universiti Sains Malaysia (USM), Penang 11800, Malaysia*
[2]*School of Electrical and Electronic Engineering, Universiti Sains Malaysia (USM), Nibong Tebal 14300, Malaysia*
[3]*Lee Kong Chian Faculty of Engineering and Science, Universiti Tunku Abdul Rahman (UTAR), Kajang 43200, Malaysia*

Correspondence should be addressed to Yung-Wey Chong; chong@usm.my

Received 9 September 2022; Revised 3 January 2023; Accepted 5 April 2023; Published 25 April 2023

Academic Editor: Abdellah Touhafi

We propose and experimentally validate a hybrid energy harvester embedded in a wearable system used to measure real-time information, such as body temperature, heartbeat, blood oxygen saturation (SpO_2), and movement (or acceleration) of human body in real time. This hybrid energy harvester, or in short eMeD, has a unique design that can improve the energy efficiency of the overall wearable system and extract more energy from ambient sources. Specifically, the wearable system is integrated with a hybrid photovoltaic-radio frequency (RF) energy harvester as the power source to prolong its lifetime and reduce the dependence on battery energy. Experimentally, the current consumption of the wearable system with load switching and event management algorithm improved from 31 mA to 18.6 mA. In addition, the maximum conversion efficiency is 14.35%. The experimental results illustrate a sustainable and long-term monitoring operation for Internet of Medical Things systems.

1. Introduction

Wearable system constitutes a new technological paradigm for Internet of Medical Things (IoMT). According to Cisco Systems [1], the number of connected wearable devices is expected to increase from 395 million in 2018 to 1,105 million in 2022. Further, IoMT growth of 21% from $72.5 billion in 2020 to $188.2 billion by 2025 has been estimated by Markets and Markets [2]. IoMT enables new creations and opportunities in the medical domain to improve the quality of people's lives while reducing healthcare cost. The creation of new application areas has changed the process in healthcare services such as data acquisition [3], clinical decision-making, and patient record management [4].

One of the critical issues in the development of IoMT is power consumption and supply in the long-term use of wearable devices [5]. To ensure user adoption, it is crucial that next-generation power sources increase the wearable device lifetime while greater functional capabilities and comfort are provided. The stagnated battery technology has prompted scientists to find ways to get the most out of their battery-powered devices. Scavenging energy from the environment is important from the viewpoint of wearable devices to reduce their dependence on battery energy [6–8]. The combination of wearable devices and the energy-harvesting technology has created opportunities. According to Brandessence, the energy-harvesting market is valued at $467.1 million in 2020 and it is expected to reach $881.7 million by 2027 [9]. In short, the challenges of IoMT are to achieve lower power requirements, use tiny devices that blend into the body, and reduce maintenance.

To provide a reliable power source containing a large energy density, the power management system of the wearable device must optimize energy conversion and deliver high efficiency and reliable energy. For outdoor applications, solar energy generally offers the best achievable energy density, but it is too dependent of the environment whereby it has energy shortage during night time. With the upsurge

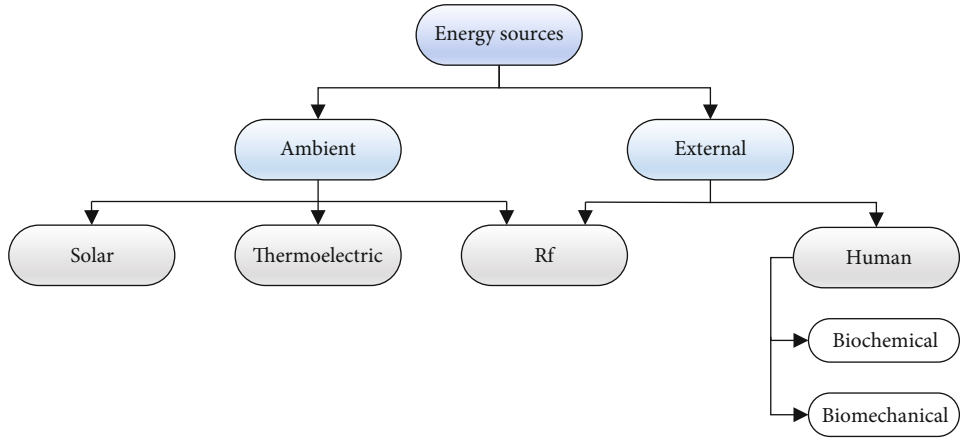

Figure 1: Energy sources for wearable systems [10].

of radio frequency (RF) applications, there has been a strong interest in the RF energy-harvesting technique. Because solar and RF sources are not available at a stable level at all times, it is necessary to design the power management system properly so that the wearable devices can draw power from multiple sources to increase its power availability.

The focus of this research is to design an effective energy-harvesting solution extracting energy from hybrid sources for wearable systems. The combination of hardware and software (i.e., the power management system) can form high-efficiency and sustainable energy supply for wearable systems. Specifically, this research integrates the low-power and state-retentive shutdown mechanism, aggressive power management, and high-efficiency environmental energy conversion into a single wearable system.

There are two main contributions in this research:

(1) An autonomous wearable system powered by hybrid energy. Solar and RF energy harvesters are used to maximize energy harvested so that the wearable system can be used in both indoor and outdoor environments. Due to the novelty of the proposed method, users do not need to consider the illumination effect of the environment

(2) An event-driven sensor management algorithm to preserve energy and meet the requirement of IoMT such as real-time tracking of patients' vital sign

2. Related Work

An energy harvester converts and stores energy from the ambient source to provide continuous power supply to electronic systems, including wearable systems. The energy source can be converted to electrical energy using transducers or converters. The energy sources can be classified into two broad categories, namely, ambient and external sources, as shown in Figure 1 [10]. Ambient sources, such as solar power, thermoelectric power, and RF are available in the surroundings at almost no cost. The characteristics of various ambient sources are unique in terms of predictability, controllability, and conversion efficiency [11]. This is because these sources are affected by time, location, and weather conditions. In contrast, external sources emit energy to the environment with the intent for the energy to be harvested by energy-harvesting system. Such energy sources are predictable and controllable because they are deployed explicitly in the environment.

To add the diversity of energy sources, several hybrid energy-harvesting systems have been proposed in the literature.

Saraereh et al. [12] propose an energy-harvesting protocol that harvests energy from 2.4 GHz RF energy and thermoelectric energy for a network of healthcare devices. The hybrid energy harvester has shown to increase network lifetime by 24% compared to a network without using any energy harvester. Colomer et al. [13] propose the integrated power conditioning circuit, which is designed using the 0.13 μm technology and a full-wave NMOS rectifier, to harvest biomechanical and solar energy. Simulation results show that the rectifier achieves an average efficiency of around 70%.

Mohsen et al. [14] propose a photovoltaic-thermoelectric hybrid energy harvester for wearable systems. The harvester provides energy to power temperature, heartbeats, and accelerator sensors. Nevertheless, the system uses the Bluetooth Low Energy (BLE) module as wireless communication, which is power hungry, to increase the lifetime of the sensor system up to 46 hours only. Zhang et al. [8] propose a hybrid RF-solar energy-harvesting systems that utilise transparent multiport micromeshed antennas for indoor applications. The integration of transparent antennas with photovoltaic (PV) cells has shown to enhance transparency and conductivity. The transparent approach allows space saving since the antenna can be integrated with solar panel and at the same time achieve good antenna efficiency.

Yu et al. [15] propose a flexible transparent antenna with flexible transparent rectifying circuit and an amorphous PV cell. The flexible antenna shows an impedance matching bandwidth of 3.5-3.578 GHz and 4.79-5.09 GHz. The transparent stacked structure enables the wearable device to achieve a higher RF-to-DC conversion efficiency at 13 dBm RF input power. Although it is designed for wearable system, the proposed system has not been tested

Table 1: Comparison between different wearable systems with its characteristics.

Reference	Methodology	Energy sources	Power management	Energy preservation algorithm
[12]	Using simulator to simulate performance of hybrid energy-harvesting protocol	RF and thermoelectric	Conceptual (simulated)	NA
[13]	Integrated power conditioning using 0.13 μm technology and full-wave NMOS rectifier to harvest biomechanical and photovoltaic energy	Biomechanical and photovoltaic	Conceptual (simulated)	NA
[14]	Wearable system that measures vital signs and powered using hybrid energy	Photovoltaic and thermoelectric	Simple DC-DC boost converter	NA
[8]	Using transparent multiport micromeshed antennas	Photovoltaic and RF	Parallel DC-DC boost converter	NA
[15]	Flexible transparent antenna with transparent rectifying circuit and photovoltaic cell	Photovoltaic and RF	ADP5091 only	NA
Proposed eMeD	Wearable system that measures vital signs and powered using hybrid RF and photovoltaic energy	Photovoltaic and RF	ADP5091 with load switch	Yes

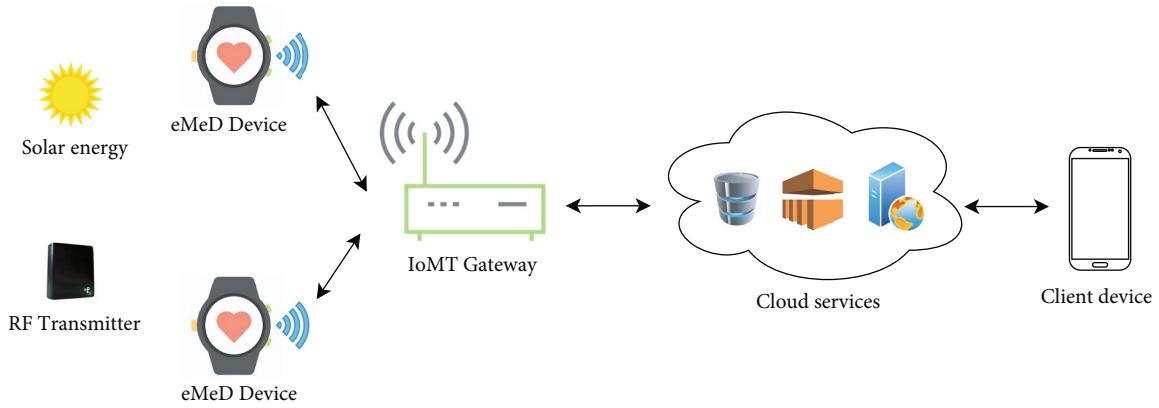

Figure 2: The overall eMeD system.

in actual IoMT environment. The design does not include wearable sensors, and the RF electromagnetic power density is artificially adjusted.

Table 1 shows the comparison between different wearable system with its characteristics.

3. Proposed System Design

Figure 2 presents the overall eMeD system. The eMeD system consists of wearable eMeD devices embedded with vital sign sensors, such as heart rate, temperature, and accelerometer. The eMeD devices are embedded with sensors with a low-power wireless communication module and a hybrid energy harvester. One of the innovations of this system is that the energy harvester is robust against changes of the environment. Specifically, the system consists of a PV panel to harvest energy from the irradiance of sunlight and a RF submodule to harvest energy from external RF. The combination of solar energy and RF energy is exploited to provide a stable energy source to the wearable system from predictable RF energy source and unpredictable solar energy source. In the power management unit, the maximum power point tracking and closed-loop voltage feedback control are used to achieve the highest possible total output power from different energy-harvesting subsystems. Specifically, the input impedance of two different converters is tuned dynamically to optimize the output power transferred from different energy-harvesting sources to the wearable device under a wide range of operating conditions. In addition, the power management unit, which operates at an input voltage spanning from 80 mV to 3.3 V, provides efficient conversion. Specifically, it has a minimum operation threshold whereby a specific condition can trigger a boost shutdown. For example, when solar energy harvester detected low light condition, an efficient power management helps to prolong the battery life and increase the life of wearable devices.

To maximize power efficiency, task execution is optimized in wearable eMeD devices using software. The eMeD device transmits sensing outcomes to an IoT gateway using the ZigBee technology. Conventionally, wearable devices are directly connected to mobile phones via BLE, but it consumes a high amount of energy, making it unsuitable for IoMT applications. The fast duty cycling is implemented in ZigBee, making the eMeD device to consume low power. There are two different profiles, namely, *sleep end nodes*

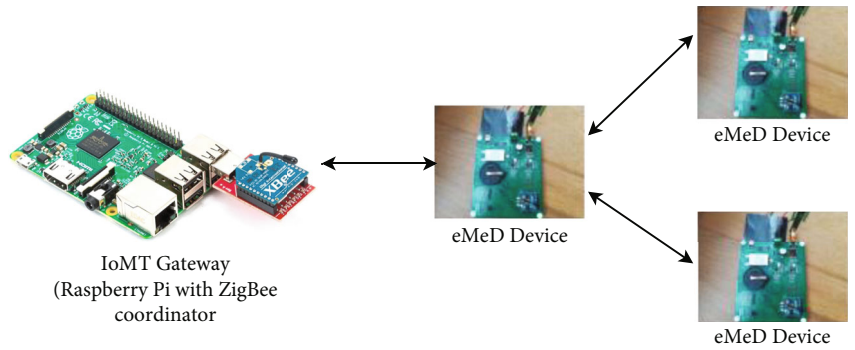

Figure 3: Wireless sensor network in eMeD.

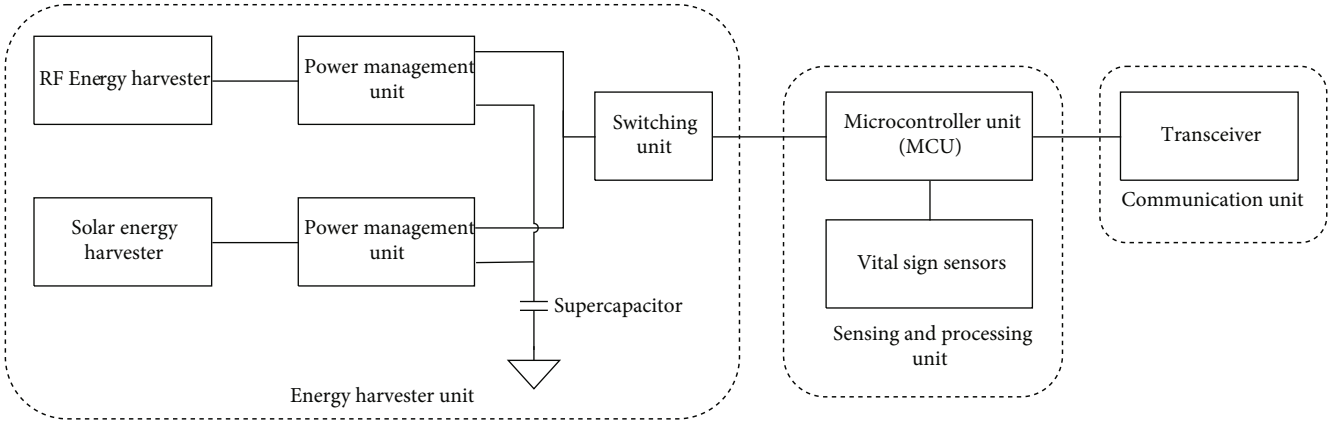

Figure 4: eMeD hardware design.

and *line-powered nodes*. Firstly, a sleep end node performs power management by means of duty cycling with two main states, namely, *hibernation* and *transmission*. A node is inactive in the hibernation state. A node is active in the transmission state. During the transmission state, the hardware abstraction layer is activated, and peripherals such as sensors and microcontroller are enabled for data collection. The node's radio uses carrier collision avoidance to ensure that a channel is available, sends data, and then switches to the sleep mode. Secondly, a line-powered node does not perform power management by means of duty cycling because the node is always awake to act as both parent and end node. Instead, the node uses software optimization to minimize the data transmission time, reduce power consumption, and optimize the power generated by energy harvesters. In contrast to many existing systems in the market, eMeD focuses on achieving an ultralow power in self-sustainable devices. WSN is integrated into eMeD devices so that they can send data to neighboring nodes, which can relay it to the IoT gateway, when patients move to different rooms or areas in a building and become disconnected from the IoT gateway.

In the eMeD system, an IoMT gateway is implemented using Raspberry Pi to handle IoMT devices and filter, preprocess, and encrypt data in the local stage as illustrated in Figure 3. Simple actions are performed at the IoMT gateway because this can reduce the bandwidth required for transmitting a large volume of data to the cloud server. An integrated application layer at the cloud server is also implemented to store a large amount of data and process it so that the data can be visualised in the mobile and web applications. This enables medical practitioners to interact with the platforms. A lightweight messaging protocol (MQTT) is used in the application layer because of its capabilities in providing different quality of service (QoS) levels, message persistence, and multicasting.

This paper presents the embodiment of technologies, including hardware and software, for building a new embedded system as part of the Internet of Medical Things. eMeD makes up for the shortcomings of using numerous cables and cords in the hospital while improving communication efficiency between medical practitioners and patients.

3.1. Hardware Design. eMeD has three subsystems, namely, the sensing and processing unit, the communication unit, and the energy harvester unit, as illustrated in Figure 4.

3.2. Sensing and Processing Unit. The sensing and processing unit consists of a microcontroller unit (MCU) and three (3) on-board sensors, namely, temperature sensor, heart rate sensor, and accelerometer. The core of the sensing and processing unit is the ATMEGA3028P-based MCU that is used to collect and process sensor data. The MCU is also used to run the event-driven sensor management algorithm to reduce the overall power consumption. The low-power, low-cost, and high-performance MCU is

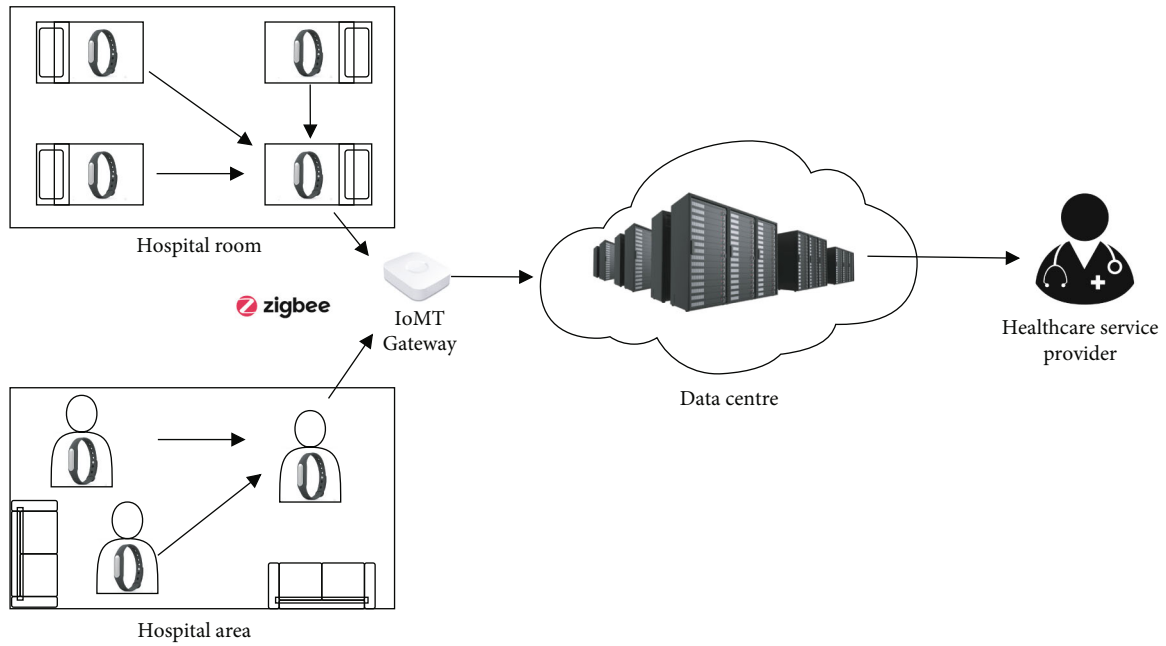

Figure 5: eMeD system deployment in IoMT setting.

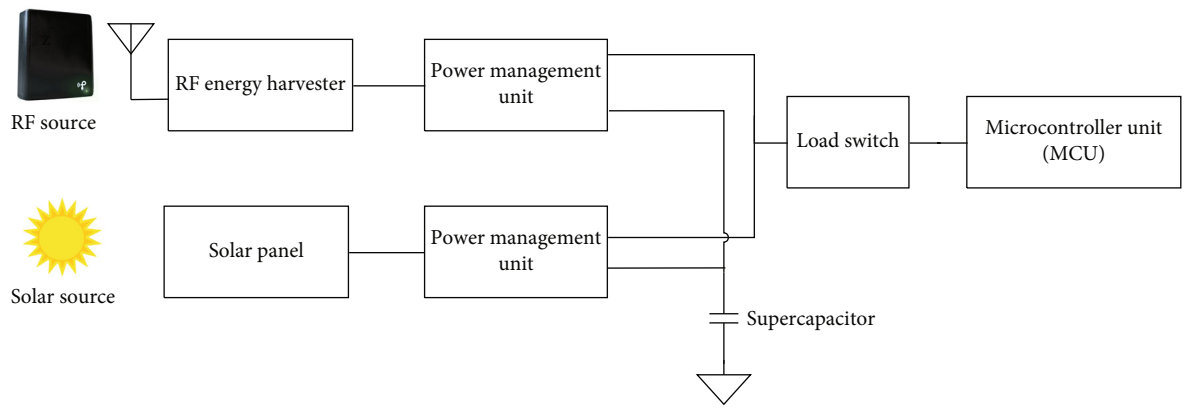

Figure 6: Energy harvester unit embedded in eMeD.

configured to 8 MHz at 3.3 V, and it can be throttled down to 1 MHz at 1.8 V for extremely low-power applications. The MCU has a 32 KB flash memory with a 2 KB SRAM, 6 analog input pins, and 14 digital I/O pins, which are connected to on-board sensors. It also comes with 16 MHz oscillators onboard.

Low-power temperature sensor (MAX30205) [16] is integrated to the eMeD device to measure skin temperature, which is one of the most fundamental monitoring measurements of patients. Intrinsic factors, such as infection or metabolic disturbances, can cause temperature instability in patients. The temperature data is sent to the MCU via the I^2C serial interface. It has a very low power consumption with a typical operating current of 600 μA and supply voltage of 3.0 V. A photoplethysmograph (PPG) heart rate sensor (MAX30102) is also connected to the eMeD device to monitor a patient's heart rate and peripheral capillary oxygen saturation (SpO_2). The PPG sensor measures changes in blood vessel contraction and expansion using LEDs and photodiodes. As arterial pulsations fill the capillary bed, the volumetric changes of the blood vessels modify the absorption, reflection, or scattering of the incident lights, such that the resultant reflective and transmittal lights represent the timing of cardiovascular events, including heart rate and oxygen saturation [17].

A 3-axis microelectromechanical system (MEMS) accelerometer (ADXL362) [18] is integrated into eMeD device so that it can capture motion rhythms used for artifact removal. ADXL362 is an ultralow power sensor that consumes (a) less than 2 μA when the output data rate is 100 Hz and (b) only 270 nA when it is in the motion-triggered wake-up mode, which has an adjustable threshold of the sleep/wake motion activation. It utilises capacitive sensing to sense the displacement of the proof mass, which is proportional to the applied acceleration. Therefore, the presence of acceleration above a threshold for a specified time period represents a motion (or activity), and the motion remains until there is a lack of acceleration above the threshold. In this project, the

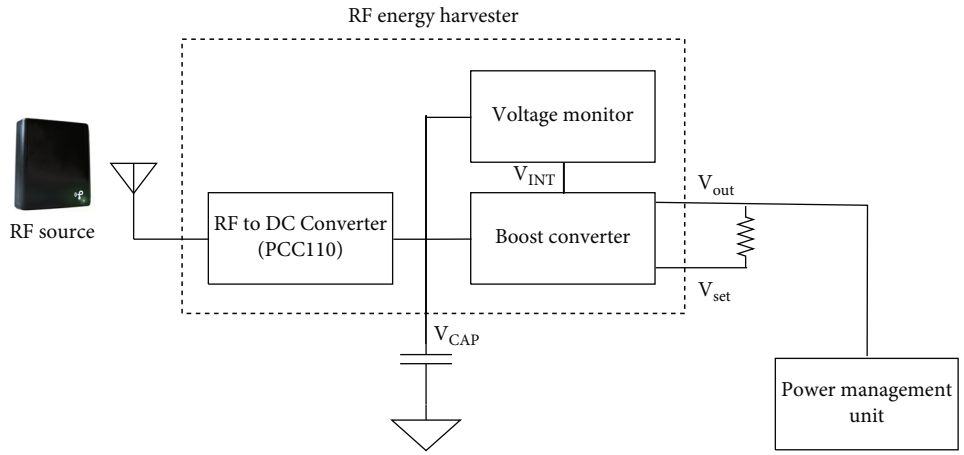

Figure 7: Block diagram of RF energy harvester in eMeD.

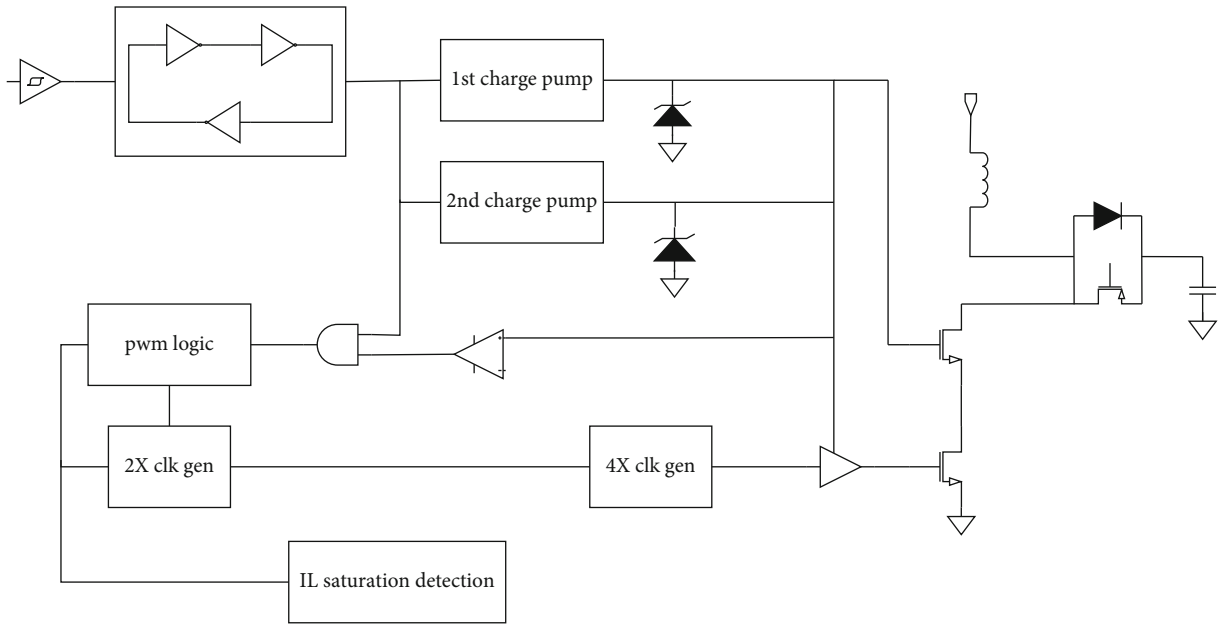

Figure 8: Power management unit [22].

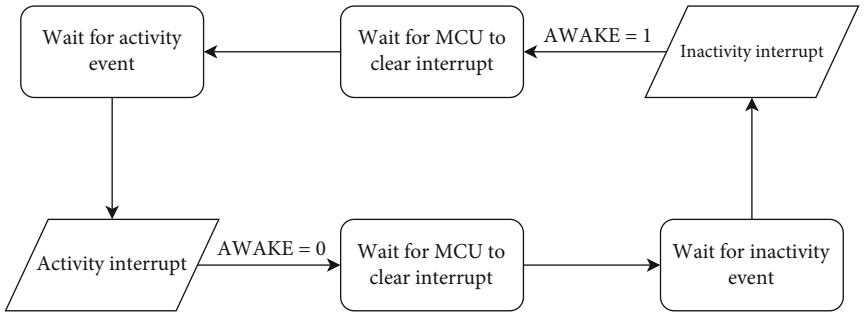

Figure 9: Flowchart illustrating activity and inactivity operation of accelerometer that is utilised in the event-driven sensor management algorithm.

motion-triggered wake-up mode is used to detect the presence of motion at extremely low power consumption of 270 nA at a supply voltage of 2.0 V. Using the motion-triggered wake-up mode allows the eMeD device to be switched off and powered down until activity is detected. The accelerometer measures acceleration only about six times per second to determine whether motion is present. When a motion is detected, the accelerometer (a) switches

into the full bandwidth measurement mode, (b) triggers an interruption signal called the AWAKE bit to MCU, and (c) wakes up downstream circuitry based on the configuration. In the wake-up mode, all accelerometer features are available except the activity timer. All registers can be accessed, and real-time data can be read and/or stored through FIFO. Such activity and inactivity detection using accelerometer can be used to trigger the wake-up mode of the heart rate and temperature sensors.

3.3. Communication Unit. To help the healthcare service provider in obtaining data from eMeD devices, a ZigBee transceiver transmits the sensor data of a patient to an IoMT gateway through wireless communication. The ZigBee-based module XBee-Pro, which follows the IEEE 802.15.4 standard for the RF module, enables a low-cost and low-power WSN. The ZigBee module is built with Silicon Labs EM357 system-on-chip [19] that operates in the 2.4 GHz ISM radio bands and offers low latency solutions with low power. The ZigBee module is also equipped with a NXP MC9S08QE32 [20] application processor that supports bootloader and controls the EM357 radio. The ZigBee module interfaces with the MCU through the universal asynchronous receiver/transmitter (UART) serial connection.

The eMeD system supports the tree configuration to increase the reliability and availability of the system. The transceiver of eMeD devices is set to the router mode whereas the transceiver of the IoMT gateway is set to the coordinator mode. The selection of different modes for the eMeD system allows the expansion of multipatient monitoring in a medical center as shown in Figure 5. eMeD devices can join an existing IoMT network and send, receive, and forward information. So, each eMeD device can act as a messenger for communication with other eMeD devices which are located outside the transmission range of the IoMT gateway. Nevertheless, to preserve the harvested energy, a separate router relays messages from one node to another node if patients are located outside the transmission range of the IoMT gateway. Unlike eMeD device that can go into the sleep mode, a ZigBee router is set up to always on mode so that it is always available for routing and forwarding packets. The IoMT gateway acts as a ZigBee coordinator to gather data from eMeD devices and forward it to the data center using TCP/IP sockets over an Ethernet network.

For data security, all data is encrypted using 128-bit symmetric encryption called AES. When new eMeD device is added to the network, AES authenticate and encrypt the data without interfering neighboring eMeD devices.

3.4. Energy Harvester Unit. To prolong IoMT operation, the energy harvester unit collects and stores a limited amount of energy extracted from two energy sources. Using two different kinds of energy sources reduces their effects to the environment condition. RF energy is used to charge the supercapacitor and operate eMeD devices when patients are inside the hospital building, and solar energy is used when patients are outside the hospital building. Such design reduces the dependence on a single energy source and the needs to manually recharge the eMeD devices. Using hybrid energy sources, the eMeD system can be deployed in both indoor and outdoor environments.

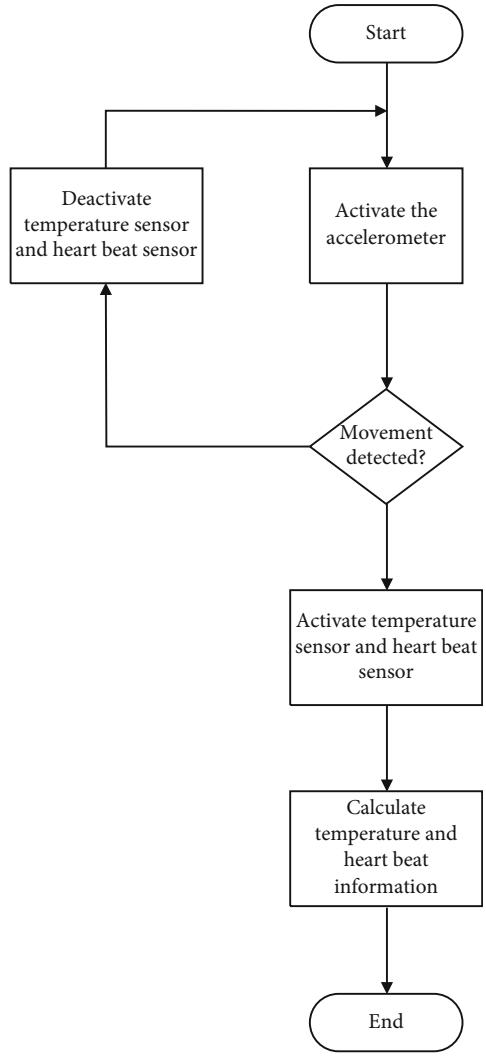

Figure 10: Event-driven sensor management algorithm to improve the accuracy of eMeD devices.

Figure 6 illustrates the block diagram of the energy harvester unit for eMeD devices. The energy harvester unit consists of two (2) power management units (PMUs), RF energy harvester, solar energy harvester, and load switch.

3.4.1. Supercapacitor. Unlike the conventional rechargeable battery-based energy storage systems that (a) require frequent periodic maintenance and (b) have limited number of recharge/discharge cycles, eMeD utilises a supercapacitor to store the harvested energy. The supercapacitors have unlimited charging cycles; thus, it can minimize the need to change the battery once it reaches the maximum number of recharge/discharge cycles. In addition, supercapacitors can minimize the environmental impact when batteries are not disposed of properly.

3.4.2. RF Energy Harvester. The RF energy harvester harvests energy from RF signals, and it consists of a RF-to-DC converter, voltage monitor, and boost converter. The RF-to-

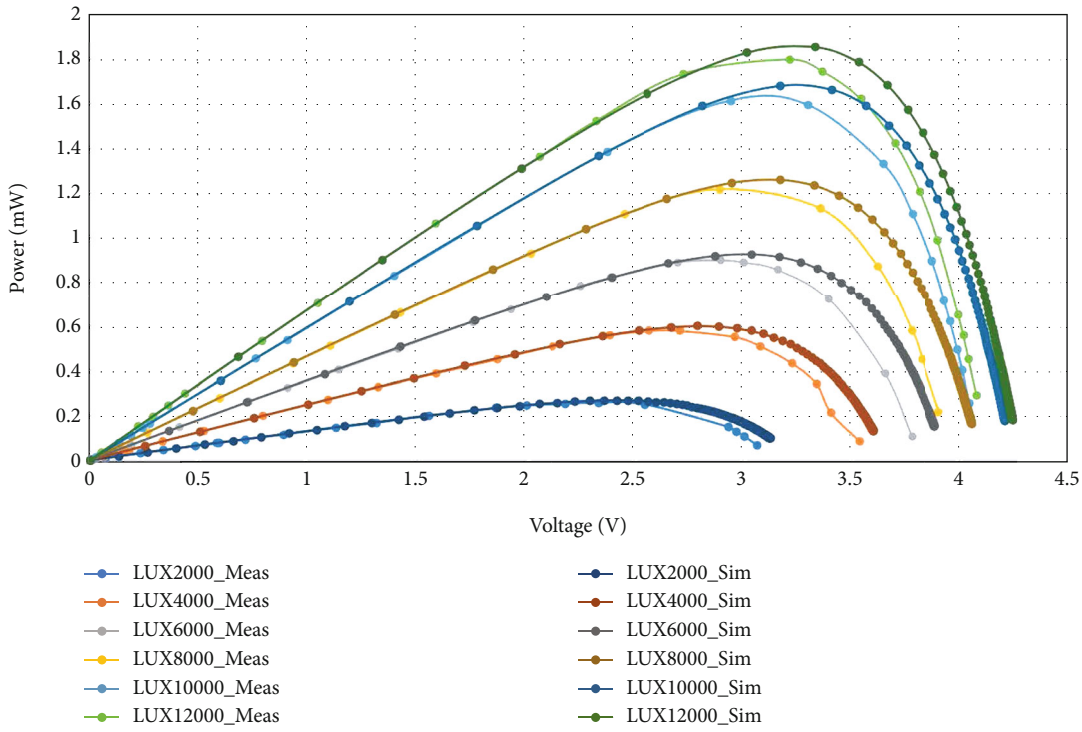

Figure 11: Output power versus output voltage using different light intensities.

Table 2: Conversion efficiencies of the photovoltaic cell.

Lux	2000	4000	6000	8000	10000	12000
Lux in mW/m^2 conversion	15.8	31.6	47.4	63.2	79.0	94.8
Input power (mW/cm^2)	0.0608	0.1217	0.1825	0.2433	0.3042	0.3650
Output power (mW/cm^2)	0.0069	0.0156	0.0241	0.0324	0.0436	0.0482
Conversion efficiency	11.40	12.81	13.18	13.31	14.35	13.19

DC-integrated circuit Powercast P2110 is used to capture energy from a 915 MHz-centered RF transmitter. RF energy reaches the RF-to-DC converter IC (PCC110) of an eMeD device as illustrated in Figure 7. Energy is stored in a capacitor connected to V_{cap} or fed to the boost converter (PCC210). The DC-DC boost converter is used to boost and regulate the output voltage of the RF rectifier. The boost converter has a default output of 3.3 V, and it can be adjusted by adding resistors to V_{set}. The impedance matching circuit maximizes the received power at the antenna, the RF-to-DC converter transforms the AC RF signals into DC voltage, and the DC-to-DC converter amplifies the DC voltage level from the RF-to-DC conversion unit to allow ultralow voltage operations. When V_{cap} reaches its maximum value, a digital line V_{INT} is set to high by the voltage monitor and the boost converter turns on, so V_{out} rises to the predetermined output voltage of the DC-DC boost converter. The supercapacitor then discharges until it reaches its minimum value, causing the voltage monitor to set the V_{INT} value to low. This causes the boost converter to switch off until the supercapacitor charges up to its maximum value. This strategy allows the RF energy harvester unit to be decoupled from the load (e.g., sensors and microcontroller) and, successively, to decouple the load from the harvester, giving the voltage regulator enough energy to be manipulated. Generally, the conversion efficiency is determined for a defined input power signal level, at a given frequency once the load impedance is specified. To have good values of this characteristic, the input RF power matching is one of the more delicate aspects in the design of the antenna-rectifier circuitry.

3.4.3. Load Switch. The load switch limits the current drawn from the supercapacitor from the harvester to ensure the current is not discharged from the supercapacitor during when energy is not harvested. Since the output voltage from the RF energy harvester depends on the amount of traffic in cellular communications or on the DTT power in the scavenging area, there is a need to control the output voltage delivered to precharge supercapacitor from the front-end circuit. The minimum voltage that the precharge capacitor needs to achieve to initiate the procedure from the buck-boost circuit is 1.8 V, whereas the maximum voltage must be no more than the voltage the supercapacitor bank is

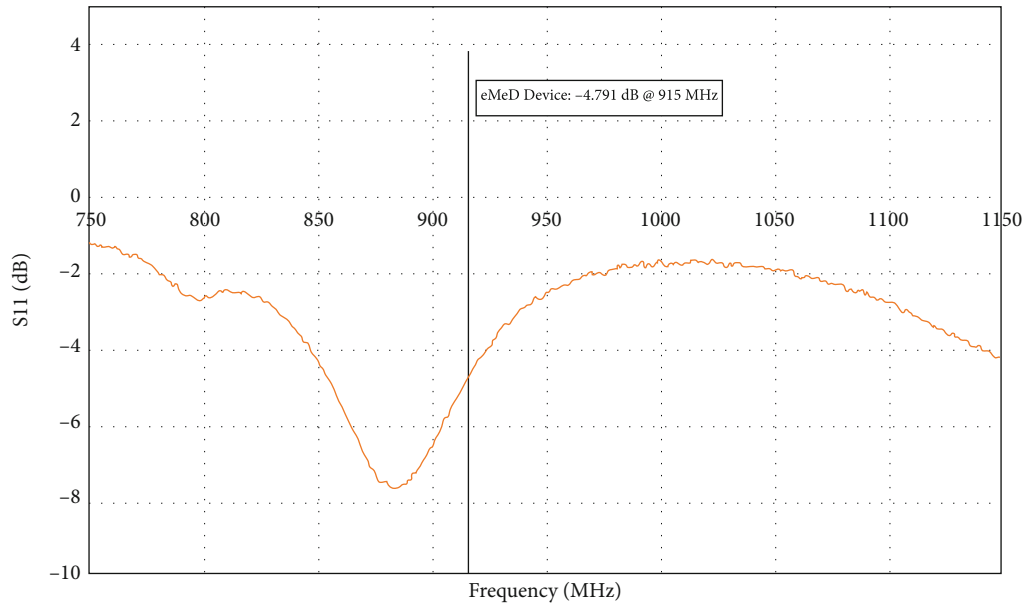

Figure 12: Return loss of eMeD device.

designed for. In terms of voltage supply, the buck-boost circuit takes a maximum tolerance of ~5%, while the maximum output ripple will be at most 2%. The RF energy is fed into the device where it reaches the RF-to-DC converter IC. There, the energy is stored in a capacitor connected to V_{CAP}.

3.4.4. Power Management Unit. An integrated circuit PMU by Analog Devices, ADP5091 [21], is connected to PV panel and RF energy harvester submodules to extract the maximum possible energy from both energy sources. The PMU integrates the maximum power point tracking circuit (MPPT) to continuously adapt the input impedance of the connected PV panels so that the maximum power can be extracted and efficiently transferred to the supercapacitor. The MPPT control keeps the input voltage ripple within a fixed range to maintain a stable DC-to-DC boost conversion. The dynamic sensing mode and no sensing mode, both programming regulation points of the input voltage, allow extraction of the highest possible energy from the harvester. It provides efficient conversion of the harvested limited power from a 6 μW to 600 mW range with submicrowatt operation losses.

An efficient energy-harvesting method is required to generate subthreshold voltage levels because the internal voltage-voltage conversion circuitry must be energized. The cold start-up circuitry in the PMU contains two charge pumps to allow the regulator to start operating at an input voltage of 380 mV as shown in Figure 8. The first charge pump controls cascading devices to protect the voltage threshold start-up switch which the second charge pump is used to make sure that the output voltage is good. The inductor saturation detection is used to minimize the start-up current. Such cold start-up circuitry design can bootstrap conversion circuits when the voltage level falls below the minimum level. As input voltage rises, the PMU disables the start-up converter and allows operations to proceed with the boost converter, which is very helpful in suboptimal situations.

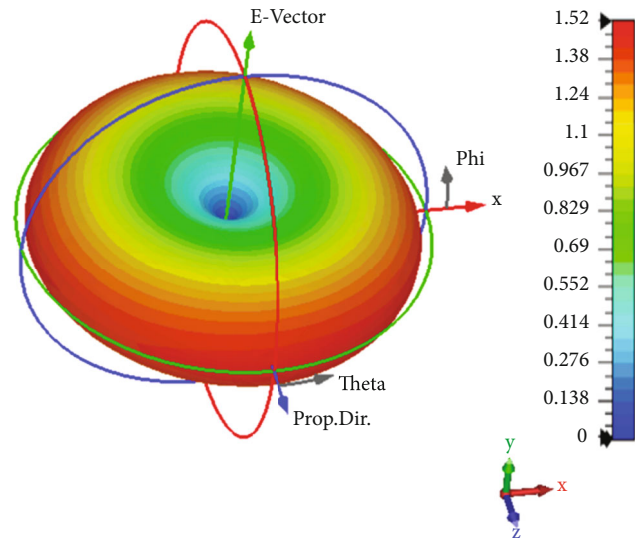

Figure 13: 3D linear radiation pattern of the designated antenna.

3.5. System Software Design. Besides hardware design, the software design plays an important role to preserve the energy of the eMeD system comprised of eMeD devices, the IoMT gateway, and WSN. The software design is separated into two (2) segments, namely, an event-driven sensor management algorithm implemented in MCU and the communication software stack in IoMT.

In eMeD devices, event-driven sensor management is implemented in the MCU. The benefit for such design is twofold. Firstly, the event-driven sensor management

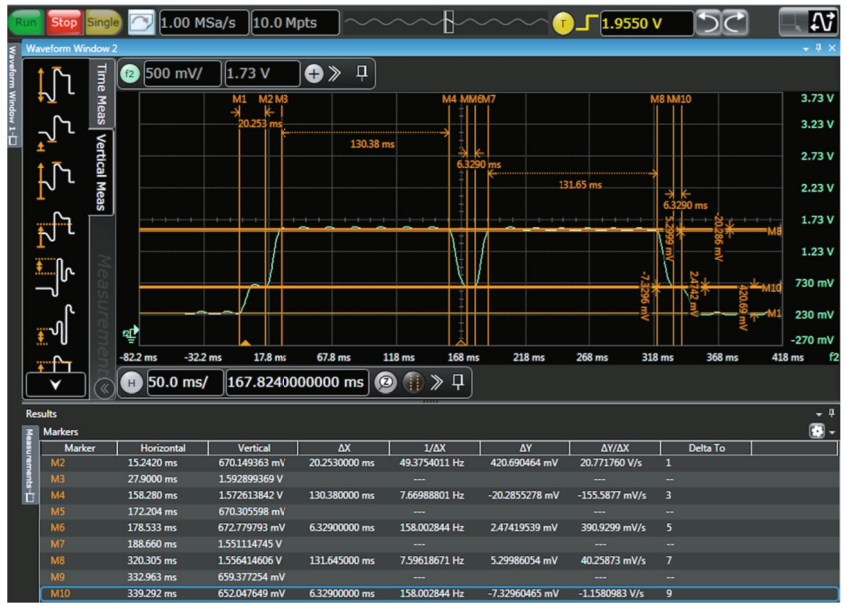

Figure 14: Current consumption of eMeD during active and idle modes.

Figure 15: Voltage of eMeD during active and idle modes with event-driven management algorithm.

algorithm assigns a minimum set of active components at any time and invokes new components only when state transitions happen. The ZigBee module spends majority of its time in the sleep mode to minimize power consumption and wakes up only when data transmission. To minimize the amount of time ZigBee wake-ups, the data acquisition and the transmission are made subsequent of each other. This can prolong the lifetime of the energy storage.

Secondly, before data can be acquired from the patient, the sensor data must be accurate. The event-driven sensor management algorithm fuses data from multiple sensors in managing sensors and providing accurate readings. PPG and temperature sensors are commonly worn on fingers which provide the strongest signal strength. Nevertheless, motion artifact due to body movements may cause temperature and heart noise estimation error [23]. Since eMeD is designed to be worn by patient, large magnitude accelerations will occur due to human movement, causing noise in the heart rate data.

In the event-driven sensor management algorithm, eMeD utilises 3-axis accelerometer to automatically recognise user's movement state before capturing vital sign data. The activity and inactivity detection functions in accelerometer are used concurrently and configured to process in the

linked mode. In the linked mode, activity and inactivity detection are linked to each other such that only one of the functions is enabled at any given time. As soon as an activity is detected, the device is assumed to be moving. Inactivity detection operates when inactivity is detected, and the eMeD device is assumed to be stationary as shown in Figure 9.

Heart rate and temperature sensors are activated when the accelerometer detects the user is in the static mode as illustrated in Figure 10. The processor operates in the active mode, but it does not activate the heart rate and temperate sensors because human movement may affect the readings of the heart rate.

4. Experimental Results and Analysis

Figure 11 shows the power-voltage characteristics of the energy harvester unit under different light intensity. The output power and output voltage are measured using a digital multimeter and light sensor to measure the lux of the light. The system is able to perform maximum power point tracking (MPPT) with the power curves achieving peak near the solar panel output voltage of 3.3 V. The maximum power point (MPP) of the solar panel is between 2.5 V and 3.5 V depending on the light intensity. This shows that the output voltage should be fixed at 3.3 V so that the maximum possible output power can be harvested from the solar panel. With the outdoor conditions being 8,000 to 10,000 lux, the maximum electrical power that the solar panel can harvest ranges from 1,200 to 1,800 μW. Figure 11 illustrates the simulated value track closely with measured value.

Table 2 shows measured conversion efficiencies of the photovoltaic cell at different input power values with solar energy harvester area of 38.5 cm^2. As shown in the table, the maximum conversion efficiency is 14.35%. The conversion efficiency is high as compared to existing work by Mohsen et al. [14] due to the efficient power management design.

As shown in Figure 12, S_{11} for an eMeD device at 915 MHz is -4.791 dB. Based on these results, the actual RF energy harvested by the embedded eMeD system is 66.9% of the incident power.

Figure 13 shows the far-field 3D radiation pattern of the designed dipole antenna at 915 MHz that is used in the hybrid energy harvester. The antenna is perfectly omnidirectional with a linear gain of 1.52 and a peak realized gain of 1.82 dBi at 915 MHz. The radiation from the RF antenna decreases to zero along its axis, as is typical for any dipole antenna. The radiation pattern envelope of points with identical radiation intensities for a doughnut-like form, with the antenna axis flowing through the hole in the middle of the doughnut, which is comparable to an omnidirectional antenna, may be seen in the three-dimensional graphic. When the source outputs unbalanced power, the sleeve balun in the antenna removes impedance mismatches.

Oscilloscope and current sense amplifier are used to verify the overall current consumption. The sensing resistor value is 0.1 Ω. For this measurement, the sensing resistor value of 0.1 Ω was selected to minimize voltage drop across it, and the selected current sense amplifier has gain of 500 V/V. In this case, the constant multiplier is equal to 0.1*500 = 50 V/A. The oscilloscope plot without event-driven sensor management algorithm is show in Figure 14. The idle current is 245.92 mV/50 V/A = 4.92 mA, busy current = 707.28 mV/50 V/A = 14.14 mA, and transmit current = 1.55 V/50 V/A = 31 mA.

When event-driven management algorithm is used, voltage for the eMeD system dropped as illustrated in Figure 15. Since the oscilloscope probe used for this testing is N2873A 10:1, the actual reading is attenuated by 10 times. Thus, the constant multiplier reduced to 5 V/A. During the idle state, the current consumption is 32.25 mV/5 V/A = 6.45 mA, busy current = 84.49 mV/5 V/A = 16.90 mA, and transmit current = 93 mV/5 V/A = 18.6 mA. This shows that the power consumption improved when event-driven management algorithm is used, making it attractive for IoMT application.

5. Conclusions

This research presents a sustainable photovoltaic-radio frequency PV-RF hybrid energy harvester, and it has been successfully developed and implemented for a self-powered IoMT system. The proposed harvester is implemented to enable eMeD to operate autonomously. The experimental results illustrate the sustainable and long-term monitoring operation for Internet of Medical Things systems through monitoring body temperature, heart rate, SpO_2, and acceleration. The system can be used in both indoor and outdoor environments, making it ideal for IoMT applications.

Data Availability

The experimental data used to support the findings of this study are available from the corresponding author upon request.

Conflicts of Interest

The authors declared that they have no conflicts of interest regarding this work.

Acknowledgments

The research project is funded by the USM RUI grant (1001/PNAV/8014078) and USM external grant (304/PNAV/6501023/U157).

References

[1] Cisco, "Cisco annual internet report (2018-2023)," 2020, https://www.cisco.com/c/en/us/solutions/collateral/executive-perspectives/annual-internet-report/white-paper-c11-741490.html.

[2] Markets & Markets, "IoT in healthcare market by component, application, end user, and region global forecast to 2025," 2020, https://www.marketsandmarkets.com/Market-Reports/iot-healthcare-market-160082804.html.

[3] K. Saleem, I. S. Bajwa, N. Sarwar, W. Anwar, and A. Ashraf, "IoT healthcare: design of smart and cost-effective sleep quality monitoring system," *Journal of Sensors*, vol. 2020, Article ID 8882378, 17 pages, 2020.

[4] F. Al-Turjman, M. H. Nawas, and U. D. Ulusar, "Intelligence in the Internet of medical things era: a systematic review of current and future trends," *Computer Communications*, vol. 150, pp. 644–660, 2020.

[5] A. A. Thabit, F. A. Al-Mayali, and Q. H. Abbasi, "WBSN in IoT health-based application: toward delay and energy consumption minimization," *Journal of Sensors*, vol. 2019, Article ID 2508452, 14 pages, 2019.

[6] S. Zhu, Z. Fan, B. Feng et al., "Review on wearable thermoelectric generators: from devices to applications," *Energies*, vol. 15, no. 9, p. 3375, 2022.

[7] S. Niu, X. Wang, Y. Fang, S. Z. Yu, and L. W. Zhong, "A universal self-charging system driven by random biomechanical energy for sustainable operation of mobile electronics," *Nature Communications*, vol. 6, no. 1, p. 8975, 2015.

[8] Y. Zhang, S. Shen, C. Y. Chiu, and R. Murch, "Hybrid RF-solar energy harvesting systems utilizing transparent multiport micromeshed antennas," *IEEE Transactions on Microwave Theory and Techniques*, vol. 67, no. 11, pp. 4534–4546, 2019.

[9] Brandessense, "Energy harvesting system market by technology (light energy harvesting, vibration energy harvesting, electromagnetic/radio frequency (RF) energy harvesting, thermal energy harvesting), by component (transducers, PMIC, secondary batteries), by application (building & home automation, consumer electronics, industrial, transportation, security), industry analysis, trends, and forecast, 2022-2028," 2021, https://brandessenceresearch.com/energy-and-mining/energy-harvesting-market-size.

[10] Y.-W. Chong, W. Ismail, K. Ko, and C.-Y. Lee, "Energy harvesting for wearable devices: a review," *IEEE Sensors Journal*, vol. 19, no. 20, pp. 9047–9062, 2019.

[11] M. L. Ku, W. Li, Y. Chen, and K. J. Ray Liu, "Advances in energy harvesting communications: past, present and future challenges," *IEEE Communications Surveys & Tutorials*, vol. 18, no. 2, pp. 1384–1412, 2016.

[12] O. A. Saraereh, A. Alsaraira, I. Khan, and B. J. Choi, "A hybrid energy harvesting design for on-body internet-of-things (IOT) networks," *Sensors*, vol. 20, no. 2, p. 407, 2020.

[13] J. Colomer, J. Brufau, P. Miribel, A. Saiz-Vela, M. Puig, and J. Samitier, "Novel autonomous low power VLSI system powered by ambient mechanical vibrations and solar cells for portable applications in a 0.13 μ technology," in *2007 IEEE Power Electronics Specialists Conference*, pp. 2786–2791, Orlando, FL, USA, 2007.

[14] S. Mohsen, Z. Abdelhalim, and Y. Khaled, "A self-powered wearable wireless sensor system powered by a hybrid energy harvester for healthcare applications," *Wireless Personal Communications*, vol. 116, no. 4, pp. 3143–3164, 2021.

[15] B.-Y. Yu, Z.-H. Wang, L. Ju et al., "Flexible and wearable hybrid RF and solar energy harvesting system," *IEEE Transactions on Antennas and Propagation*, vol. 70, no. 3, pp. 2223–2233, 2021.

[16] I. Maxim, "Human body temperature sensor," 2016, https://datasheets.maximintegrated.com/en/ds/MAX30205.pdf.

[17] I. Maxim, "High-sensitivity pulse oximeter and heart-rate sensor for wearable health," 2015, https://datasheets.maximintegrated.com/en/ds/MAX30102.pdf.

[18] D. Analog, "Micropower, 3-axis, ±2 g/±4 g/±8 g digital output MEMS accelerometer," 2018, https://www.analog.com/media/en/technical-documentation/data-sheets/ADXL362.pdf.

[19] L. Silicon, "EM351/EM357 high-performance, integrated ZigBee/802.15.4 system-on-chip," 2013, https://www.silabs.com/documents/public/data-sheets/EM35x.pdf.

[20] S. Freescale, "MC9S08QE32 series covers: MC9S08QE32 and MC9S08QE16," 2011, https://www.nxp.com/docs/en/data-sheet/MC9S08QE32.pdf.

[21] D. Analog, "Ultralow power energy harvester PMUs with MPPT and charge management," 2017, https://www.analog.com/media/en/technical-documentation/data-sheets/ADP5091-5092.pdf.

[22] B. Chen, "Introduction to energy harvesting transducers and their power conditioning circuits," in *Low-Power Analog Techniques, Sensors for Mobile Devices, and Energy Efficient Amplifiers*, pp. 3–12, Springer, 2019.

[23] J. Shin and J. Cho, "Noise-robust heart rate estimation algorithm from photoplethysmography signal with low computational complexity," *Journal of Healthcare Engineering*, vol. 2019, Article ID 6283279, 7 pages, 2019.